On the Use of Cavity Modes as Basis Functions in the Full Wave Analysis of Printed Antennas

Giuseppe Vecchi, *Member, IEEE,* Paola Pirinoli, *Member, IEEE,* and Mario Orefice, *Member, IEEE*

***Abstract*— Magnetic wall cavity (MWC) modes are often employed as basis functions in the method of moments (MoM) full wave analysis of printed antennas, especially in its spectral domain version, where the use of entire domain basis functions is particularly convenient, but in some cases the TE (solenoidal) modes are not included. Here we investigate on the effect of this exclusion, explaining the nature of the TE-TM coupling, presenting criteria to determine the necessary number of modes, and giving numerical results for annular patches, especially relevant in this context.**

***Index Terms*—Cavity modes, full-wave analysis, printed antennas.**

I. Introduction

In the analysis of printed antennas with the integral equation (EFIE) approach, the use of appropriate entire-domain basis functions is often convenient, because few of such terms are sufficient to well represent the solution. Entire-domain basis functions are almost always associated with the spectral domain version of the method of moments (MoM): this implies that the two-fold Fourier transform (FT) of the basis/test functions has to be known in a form that allows a fast numerical evaluation.

Since a patch antenna approximately behaves like a magnetic wall cavity (MWC), the modes of this cavity are often employed to generate the basis functions for the surface current on the patch. The MWC modes are readily available for several separable geometries (rectangular, circular, annular, triangular, $\cdots$) and often also their FT can be found in convenient form; recently, a generalization of these modes has also been introduced by the authors [1], [2] to deal with arbitrary shapes and include the field singularity at the edge.

In the following we indicate (as usual) by TM the modes with zero surface curl on the patch, and by TE (solenoidal) those with zero surface divergence. To have a complete basis, both TM and TE modes must obviously be considered. However, in the literature about printed antennas, often (although with some exceptions [3]) only the TM modes are considered, this seeming the rule in the case of ring radiators [4]–[8]. In the following, we will investigate on the effects of this approximation; while the rationale for neglecting TE modes is probably the TM dominance of the resonance modes, it will be shown that this omission may lead to inaccurate results. As explained in Section II, the TE-TM coupling is generated by the edge of the metallizations: in Sections III and IV substantiate the general discussion is substantiated with numerical results for an annular patch. We have chosen this configuration because in literature its analysis is often carried out with MWC modes, but (as mentioned before) to the best of our knowledge, only TM modes are taken in account. On the other hand, when printed rings are employed in frequency selective surfaces, both TM and TE modes are considered [9].

Although in this work we will discuss numerical result only for a free-standing annular patch, the formulation is carried out for an arbitrary geometry and the conclusions obtained therefrom are of general validity.

Manuscript received November 13, 1996; revised Novbember 25, 1997.

The authors are with the Politecnico di Torino, Dip. di Elettronica, I-10129 Torino, Italy.

Publisher Item Identifier S 0018-926X(98)02687-8.

II. Reaction Integrals and TE-TM Coupling

A key point in the MoM analysis is the computation of the reaction integrals between the basis functions, here denoted by $\underline{B}_n$: we will be ultimately concerned with this computation in the spectral domain $\underline{k}_t$, where the transformed functions are denoted by a tilde ($\underline{\tilde{B}}_n$); a Galerkin testing scheme will be assumed throughout. For a transversally infinite dielectric, stratified along the axis $\hat{z}$, the spectral dyadic Green's function is diagonal in the polar basis identified by the polar unit vectors $\hat{k}_t$ and $\hat{\alpha} = \hat{z} \times \hat{k}_t$ (e.g., [10])

$$\underline{\underline{\tilde{G}}}(k_t) = \hat{k}_t \hat{k}_t \, g^{\mathrm{TM}}(k_t) + \hat{\alpha}\hat{\alpha} \, g^{\mathrm{TE}}(k_t) \tag{1}$$

where the two scalar functions $g^{\mathrm{TE}}(k_t), g^{\mathrm{TM}}(k_t)$ can be found by solving equivalent transmission line problems and take into account the characteristics of the dielectric stratification; the reaction integrals in the spectral domain can therefore be written as

$$Z_{mn} = \frac{1}{4\pi^2}\{\langle \hat{k}_t \cdot \underline{\tilde{B}}_m, g^{\mathrm{TM}} \, \hat{k}_t \cdot \underline{\tilde{B}}_n \rangle + \langle \hat{\alpha} \cdot \underline{\tilde{B}}_m, g^{\mathrm{TE}} \, \hat{\alpha} \cdot \underline{\tilde{B}}_n \rangle\} \tag{2}$$

so that only the projections of the transformed basis functions along the two polar directions $\hat{k}_t$ and $\hat{\alpha}$ are needed. Following an approach similar to that introduced by Amitay and Galindo [11] for a different problem (but never used before for printed antennas) we rearranged the spectral MoM to evaluate those projections directly from their spatial counterparts, strongly reducing the complexity of the required FT [12]. This treatment is valid for any stratification, and for a patch occupying a surface Σ of arbitrary form delimited by the curve $\Gamma : \underline{\rho} = \underline{\rho}_\Gamma$. The relevant geometrical quantities are depicted in Fig. 1: $\hat{\nu}$ and $\hat{s} = \hat{z} \times \hat{\nu}$ are normal and tangential directions on Γ, respectively.

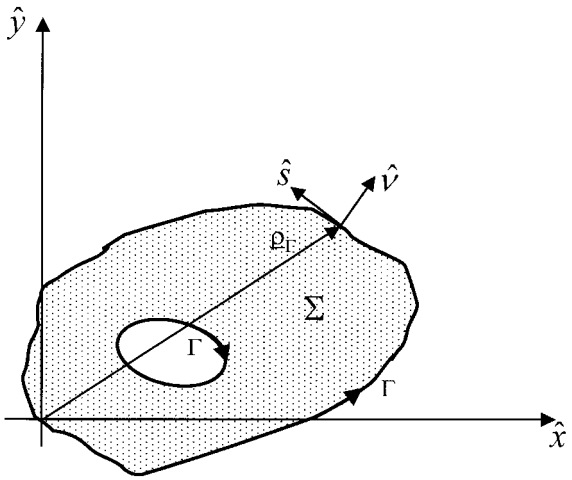

Fig. 1. Geometry for a patch of arbirtrary shape.

The basis functions $\underline{B}$ for the surface current $\underline{J}$ must be div-conforming and subject to the condition $\hat{\nu} \cdot \underline{J}|_\Gamma = 0$, which corresponds to a PMC condition ($\hat{s} \cdot \underline{H}|_\Gamma = 0$, with $\underline{J} = \hat{z} \times \underline{H}|_\Sigma$) at the edge, and therefore the TM and TE modes of the MWC are a complete set for the unknown surface current $\underline{J}$.

The projections of the transformed basis functions $\tilde{\underline{B}}_n$ along the two polar directions are related to the FT of the divergence and curl of the basis functions, respectively [12]

$$\hat{k}_t \cdot \tilde{\underline{B}} = \frac{1}{-jk_t}(-j\underline{k}_t) \cdot \tilde{\underline{B}}(\underline{k}_t) = \frac{1}{-jk_t}\mathrm{FT}^2\{\nabla_t \cdot \underline{B}(\underline{\rho})\} \tag{3}$$

and

$$\begin{aligned}\hat{\alpha} \cdot \tilde{\underline{B}} &= \frac{1}{-jk_t}(-j\underline{k}_t) \cdot [\hat{z} \times \tilde{\underline{B}}(\underline{k}_t)] \\ &= \frac{1}{-jk_t}\mathrm{FT}^2\{\nabla_t \cdot [\hat{z} \times \underline{B}(\underline{\rho})]\}\end{aligned} \tag{4}$$

($\nabla_t \cdot [\hat{z} \times \underline{B}(\underline{\rho})]$ is equivalent to the surface curl $\hat{z} \cdot [\nabla_t \times \underline{B}]$).

To explicitly enforce the condition that the basis functions $\underline{B}_n$ must vanish outside the conductor surface Σ, we write $\underline{B}_n(\underline{\rho}) = W_\Sigma(\underline{\rho})\, \underline{f}_n(\underline{\rho})$, where $W_\Sigma(\underline{\rho}) = 1$ on Σ and zero elsewhere, and $\underline{f}$ need to be defined only on Σ. Thus, after some manipulation [12] one finds

$$\nabla_t \cdot \underline{B}(\rho) = W_\Sigma(\underline{\rho})\, \nabla_t \cdot \underline{f}(\underline{\rho}) \tag{5}$$

$$\begin{aligned}\nabla_t \cdot [\hat{z} \times \underline{B}(\underline{\rho})] = {} & \hat{s} \cdot \underline{f}(\underline{\rho}_\Gamma)\, \delta(\underline{\rho} - \underline{\rho}_\Gamma) \\ & + W_\Sigma(\underline{\rho})\, \nabla_t \cdot (\hat{z} \times \underline{f}(\underline{\rho}))\end{aligned} \tag{6}$$

where the operator ∇_t is transverse to $\hat{z}$.

Employing the MWC modes as basis functions $\underline{f}$, the $\mathrm{TM}(\underline{f}')$ and $\mathrm{TE}(\underline{f}'')$ modes can be immediately derived by duality from the modes of the corresponding PEC waveguide, and so they can be expressed in terms of the TE and TM scalar eigenfunctions Ψ and Φ, respectively [13], with $\underline{f}' \propto \nabla_t \Psi$, $\underline{f}'' \propto \hat{z} \times \nabla_t \Phi$ (note the TE-TM exchange). The solenoidal property of the TE modes can be explicited to write $\underline{B}'' = \hat{z} \times \nabla_t \Phi$ everywhere, so that (4) for these modes can be simplified to

$$\hat{\alpha} \cdot \tilde{\underline{B}}'' = \mathrm{const.}(-\mathrm{j}k_t)\tilde{\Phi}. \tag{7}$$

Note also that the definition of the modes via $\nabla_t \Phi$, $\nabla_t \Psi$ and the Helmholtz equation allow one to easily write the $\nabla_t \cdot \underline{f}'$ and the $\nabla_t \times \underline{f}''$ terms as directly proportional to Ψ and Φ [12]. From standard considerations on the boundary conditions $\frac{\partial}{\partial \nu}\Psi|_\Gamma = 0$ and $\Phi|_\Gamma = 0$, one can see that the boundary term in (6) never vanishes for the TM modes of the MWC. Otherwise said, in this context of open structures, the TE basis functions are solenoidal, but the TM basis functions are irrotational only in a weak sense (almost everywhere): the projection of their FT on $\hat{\alpha}$ is not zero, and TE-TM coupling is always present.

Moreover, as detailed in [1], the solenoidal set of basis functions represents the edge singularity responsible for the blow out of the current parallel to the edge; this singular behavior usually affects the coupling to the feed structure, when the latter extends across the edge of the patch, as it is always the case for monolithic or electromagnetic (proximity) coupling. On the other hand, this is scarcely noticeable for the probe-fed patches, a fact that may explain the results reported so far for this case (like in [4] and [5]). While the incompleteness of a purely TM set is obvious, the considerations above allow to detail the effect of this incompleteness on the numerical solution. This will be the objective of the next sections.

III. The Ring

For an annular patch, the procedure described in Section II for the evaluation of the FT of basis functions, i.e. of MWC modes, is particularly meaningful; in fact, although the ring is a canonical, separable shape, the evaluation of the Hankel transform that arises from the two-fold FT of most reasonable basis functions proves to be a difficult task; the use of orthogonal polynomials, that can easily accommodate the edge behavior, does not lead to entirely closed-form expressions, and the evaluation of the reaction integrals is computer-intensive [14], [15]. On the other hand, the Vector Hankel Transform (VHT) method [4] allows an efficient formulation of the problem in association with MWC modes, but is confined to axial-symmetric configurations, with an extension to the probe-fed case, and a configuration with a general feed network cannot be analyzed with this technique. Instead, application of the technique in Section II will allow the use of MWC modes in the spectral domain with a general coupling geometry.

The $\mathrm{TM}(\underline{B}'_n)$ and $\mathrm{TE}(\underline{B}''_n)$ basis functions can be conveniently expressed in terms of the scalar eigenfunctions of the coaxial waveguide with PEC walls [13]; for ease of reference, in the following we will adhere to the usual notation of Marcuvitz [13, Sec. 2.4] (note the exchange of $\mathrm{TM}(')$ and $\mathrm{TE}('')$ superscripts when passing from the MWC to the dual electric-wall coaxial guide). Because of the separability of $\Psi(\rho, \phi)$, $\Phi(\rho, \phi)$, the two-fold FT of (5), (6) reduce to one Hankel (Bessel) transform, and one obtains their expressions in closed form [12]. For TM modes (corresponding to TE of

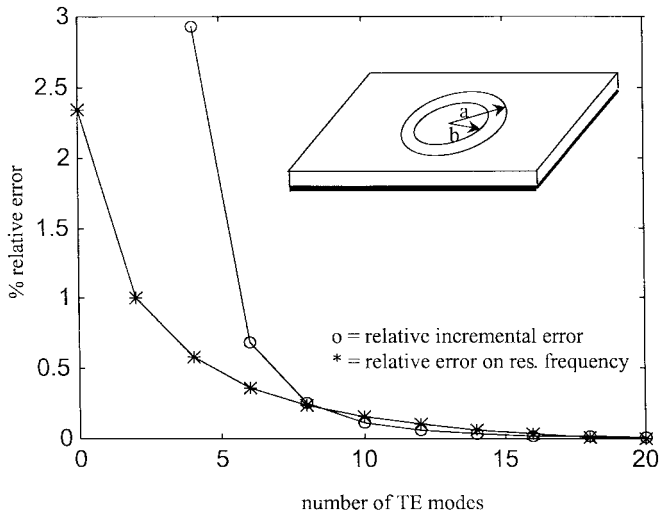

Fig. 2. Wide ring: comparison between the relative incremental error Δ_n and the relative error on the resonance frequency. Inset: ring patch geometry.

the coaxial guide)

$$\mathrm{FT}^2\{\nabla_t \cdot \underline{B}'_{mn}\} = (k''_{cmn})^2\, 2\pi(j)^m \cos(m\alpha)\, I_{mn}(k_t) \quad (8)$$

with

$$I_{mn}(k_t) \equiv \left[\frac{k_t\rho\, \mathcal{Z}_m\left(\chi'_{mn}\frac{\rho}{b}\right)J_{m-1}(k_t\rho) - \chi'_{mn}\frac{\rho}{b}\,\mathcal{Z}_{m-1}\left(\chi'_{mn}\frac{\rho}{b}\right)J_m(k_t\rho)}{\left(\frac{\chi'_{mn}}{b}\right)^2 - k_t^2}\right]^{\rho=a}_{\rho=b} \quad (9)$$

$$\mathrm{FT}^2\{\nabla_t \cdot [\hat{z} \times \underline{B}'_{mn}(\underline{\rho})]\} = 2\pi(j)^m m \sin(m\alpha) \cdot \left[\mathcal{Z}_m\left(\chi'_{mn}\frac{a}{b}\right)J_m(k_t a) - \mathcal{Z}_m(\chi'_{mn})\,J_m(k_t b)\right] \quad (10)$$

where $k_t = |\underline{k}_t|$, a and b are the outer and inner radii of the ring, respectively (see inset in Fig. 2), c is the aspect ratio $c = a/b$, χ'_{mn} is the nth root of $J'_m(a\chi'/b)N'_m(\chi') - N'_m(a\chi'/b)J'_m(\chi') = 0$, J_m and N_m are the Bessel and Neumann functions

$$k''_{cm1} = \frac{(c+1)\chi'_{m1}}{(a+b)}, \quad k''_{cmn} = \frac{(c-1)\chi'_{mn}}{(a-b)}, \quad n > 1 \quad (11)$$

and

$$\mathcal{Z}_m(\chi'_{mn}\rho) = \frac{\sqrt{\pi\epsilon_m}}{2}\,\frac{J_m\left(\chi'_{mn}\frac{\rho}{b}\right)N'_m(\chi'_{mn}) - N_m\left(\chi'_{mn}\frac{\rho}{b}\right)J'_m(\chi'_{mn})}{\left\{\left[\frac{J'_m(\chi'_{mn})}{J'_m(c\chi'_{mn})}\right]^2\left[1-\left(\frac{m}{c\chi'_{mn}}\right)^2\right] - \left[1-\left(\frac{m}{\chi'_{mn}}\right)^2\right]\right\}^{1/2}} \quad (12)$$

where $\epsilon_m = 1$ if $m = 0$ and $\epsilon_m = 2$ otherwise.

For the TE functions, $\nabla_t \cdot \underline{B}''_{mn} = 0$, while

$$-jk_t\tilde{\Phi} = -2\pi(j)^{m+1}\sin(m\alpha)k_t\,\bar{I}_{mn}(k_t) \quad (13)$$

where $\bar{I}_{mn}$ has the same expression as I_{mn} in (9), but with $\mathcal{Z}_m(\chi'_{mn}\rho)$ now replaced by

$$\bar{\mathcal{Z}}_m(\chi_{mn}\rho) = \frac{\sqrt{\pi\epsilon_m}}{2}\,\frac{J_m\left(\chi_{mn}\frac{\rho}{b}\right)N_m(\chi_{mn}) - N_m\left(\chi_{mn}\frac{\rho}{b}\right)J_m(\chi_{mn})}{\left[\frac{J_m(\chi_{mn})}{J_m(c\chi_{mn})} - 1\right]^{1/2}} \quad (14)$$

χ_{mn} is the nth root of $J_m(a\chi/b)N_m(\chi) - N_m(a\chi/b)J_m(\chi) = 0$

$$k'_{cmn} = \frac{(c-1)\chi_{mn}}{(a-b)}. \quad (15)$$

The normalization of the spatial basis functions corresponding to the above is the following:

$$\underline{f}' = -\frac{1}{k'_c}\nabla_t\Psi \quad \underline{f}'' = -\frac{1}{k''_c}\hat{z}\times\nabla_t\Phi \quad (16)$$

with [12]

$$\Psi_{mn}(\underline{\rho}) = \mathcal{Z}_m\left(\chi'_{mn}\frac{\rho}{b}\right)k''_c\cos(m\phi) \quad (17)$$

and

$$\Phi_{mn}(\underline{\rho}) = \bar{\mathcal{Z}}_m\left(\chi_{mn}\frac{\rho}{b}\right)k'_c\sin(m\phi) \quad (18)$$

IV. Results

We report here the results obtained for two configurations for which experimental data and/or other numerical results were available. These latter are obtained using Chebyshev polynomials with the appropriate edge singular behavior for the radial and azimuthal current components; the expressions of these functions and their FT are reported in the Appendix. Both the considered configurations consist of a free-standing patch, printed on a dielectric layer of thickness $h = 0.55$ mm and dielectric constant $\varepsilon_r = 2.33$. In the first case the aspect ratio $c = a/b$ is equal to two ("wide" ring), while in the other $c \simeq 1.2$ ("narrow" ring). The comparison is done for the first resonant mode, with azimuthal index $m = 1$.

In the case reported here of a free-standing patch, the two-dimensional spectral reaction integrals reduce to a single integration along the radial spectral variable k_t; we performed the integration along the real k_t axis with a contour deformation to avoid the (surface wave) poles of the Green's function.

The resonance behavior is analyzed via the SVD technique, and the resonance frequency is found as the real part of the complex frequency for which the smallest singular value $(\mathrm{SV}_{\min})$ of the impedance matrix has a zero [16].

In order to obtain an accurate representation of the solution, it is necessary to ascertain how many and what modes are needed. That can be done efficiently following a technique developed by the authors [1], [2], [17] for a more general configuration. First, the number of the (dominant) TM modes necessary to obtain a specific accuracy at a given frequency is established, then the information on the modes coupled to the selected TM is extracted from the asymptotic coupling (sub)matrices formed by the reaction integrals associated to the asymptotic behavior (for large k_t) of the spectral Green's function. These terms are frequency-independent, and correspond to the static behavior in the spatial domain.

Applying this procedure, we found that five TM terms are sufficient, in the sense that there is no sensible change (less then 0.1%) in the resonance frequency using more terms, both

for the narrow and the wide ring [18]. To determine the set of necessary modes without computation of the frequency response, one can employ the portion of the MoM impedance matrix related to the asymptotic behavior of the TM part of the Green's function, that is frequency independent. The procedure is identical to that outlined below for the TE, and its explanation deferred until then.

For the annular patch, the selection of TE modes is simpler than in the general case [1], [2], because the axial symmetry of the ring causes the odd TM modes to be coupled predominantly with the even TE modes, and vice-versa for the even TM modes, and the coupling decreases (almost monotonically) with increasing difference of the radial index n. Therefore, one can determine how many TE are needed simply proceeding in an incremental manner, i.e. adding higher indices n and checking the asymptotic, frequency independent, part of the TM-TE coupling matrix. Denoting by $[\sigma]_n$ the vector of the singular values of this coupling matrix when n TE modes are considered, we define the relative incremental error

$$\Delta_n = \frac{\|[\sigma]_n - [\sigma]_{n-1}\|_2}{\|[\sigma]_n\|_2} \tag{19}$$

and stop adding terms when Δ_n is below a given threshold. In Fig. 2, Δ_n is shown (in the case of the wide ring and of 5 TM modes), and compared with the error on the resonance frequency. This latter is defined as the relative shift of the resonance frequency with respect to the "reference" value obtained with 20 TE modes. The two curves have the same trend, proving the efficiency of the truncation criterion given above.

The effect of the TE on the resonance frequency can be appreciated in Fig. 2; further information on the resonance behavior is obtained from Fig. 3, where the magnitude of $1/\mathrm{SV}_{\min}$ is plotted versus the frequency, employing five TM modes and no TE, 5 TM + 6 TE, and six Chebyshev polynomials three for each current component, that warrant the convergence of the result). With the TM alone, a resonance frequency $f_{\mathrm{ris}} = 3.457$ GHz is found, with TE + TM one finds $f_{\mathrm{ris}} = 3.527$ GHz, and employing Chebyshev polynomials $f_{\mathrm{ris}} = 3.561$ GHz. While the relative difference in the latter two cases is below 1%, the use of TM alone shifts the resonance frequency of about 3%; although small, this error is not negligible in a structure with a bandwidth of a few percent.

As to the computational effort, even if the number of employed MWC modes is twice that of Chebyshev polynomials, the time requested for the evaluation of the reaction integrals for the MWC is sensibly smaller then that for the Chebyshev polynomials, because the FT of the MWC modes is completely in closed form.

Finally, in Fig. 4 the radial variation of the radial (top) and azimuthal (bottom) current components at the resonance is reported for an azimuthal angle $\phi = 45°$. As expected, especially the azimuthal, dominant component is drastically modified by the introduction of TE terms, because of its singular behavior at the edges. The "ripple" present in the solution is an intrinsic effect of the orthogonal nature of these entire domain basis functions, as in the mode matching technique, and is known not to create problems neither in the radiated fields, nor in the evaluation of circuit parameters, that are "variational."

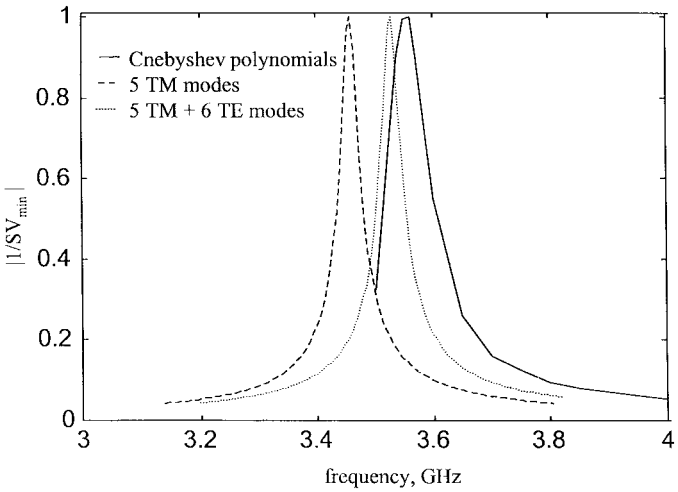

Fig. 3. Wide ring: magnitude of $1/\mathrm{SV}_{\min}$ versus the frequency; continuous line: only TM; dashed line: TM + TE; dotted line: Chebyshev polynomials.

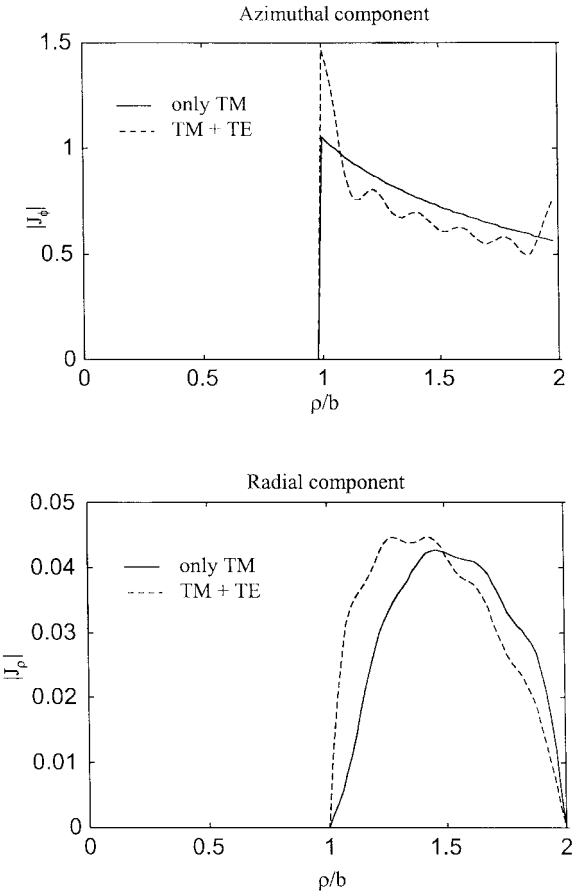

Fig. 4. Wide ring: magnitude of azimuthal and radial current components at the resonance versus ρ ($\phi = 45°$). Continuous line: only TM; dashed line: TM + TE.

For the case of the narrow ring, an analogous study has been carried out; the results on the convergence of the TE and their effects on the the resonance frequency are almost the same as the other configuration. For this configuration experimental results were also available: the measured patch has been fed

TABLE I
NARROW RING: RESONANCE FREQUENCY AND RELATIVE ERROR WITH RESPECT TO THE MEASURED VALUE

	Resonance frequency (GHz)	Per cent relative error
MWC TM modes alone	3.56	2.5%
MWC TM + TE modes	3.63	0.5%
Chebyshev polynomials	3.62	0.9%
measured data	3.65	-

by an electromagnetically coupled microstrip line, running at the same distance from the radiator and the groundplane; the distance between the line end and the ring has been arranged to obtain a low coupling, to simulate as closely as possible a free-standing patch. In Table I, the computed and measured resonance frequencies are reported; there the relative error is taken with reference to the measured resonance.

V. CONCLUSION

We have discussed the use of TE MWC modes in the full-wave analysis of printed antennas. This class of modes is sometimes neglected, in particular in the case of annular patches. The TM-TE coupling has been shown to be related to the fact that a patch is an open structure, and the further role of the TE in building up the singular edge behavior has been discussed. Numerical results for annular microstrip patches show that the neglect of TE modes produces a shift of the resonance frequency comparable to the (typically narrow) bandwidth of these structures. Criteria for the determination of the necessary number of modes have been given.

APPENDIX

The Chebyshev polynomial basis functions for the ring have the form

$$\underline{B}_{m,q,n}(\rho) = \hat{\rho}\, h_q(\rho)\cos m\phi + \hat{\phi}\, f_n(\rho)\sin m\phi \tag{20}$$

where $h_q(\rho) = \sqrt{1-x^2}U_q(x)$, $f_n(\rho) = T_n(x)/\sqrt{1-x^2}$, T_n and U_n are Chebyshev polynomial of first and second kind, respectively, and $x = (\rho - r_0)/w$, with $r_0 = (a+b)/2$ and $w = (a-b)/2$.

In the spectral domain, one finds [19]

$$\begin{aligned}\tilde{\underline{B}}_{m,q,n}(\underline{k}_t) = &\left[H_k^{(m,q)}(\underline{k}_t)\hat{k}_t + H_\alpha^{(m,q)}(\underline{k}_t)\hat{\alpha}\right] \\ &+ \left[F_k^{(m,n)}(\underline{k}_t)\hat{k}_t + F_\alpha^{(m,n)}(\underline{k}_t)\hat{\alpha}\right]\end{aligned} \tag{21}$$

where

$$F_k^{(m,n)}(\underline{k}_t) = j^{(m+1)}\frac{2m}{k_t}\cos m\alpha\, f_{m,n}^{(1)} \tag{22}$$

$$\begin{aligned}&F_\alpha^{(m,n)}(\underline{k}_t) \\ &= j^{(m+1)} w \sin m\alpha\left[\frac{1}{2}\left(f_{m+1,n+1}^{(1)} - f_{m-1,n+1}^{(1)}\right)\right. \\ &\quad \left. + \frac{1}{t}\left(f_{m+1,n}^{(1)} - f_{m-1,n}^{(1)}\right) + \frac{1}{2}\left(f_{m+1,n-1}^{(1)} - f_{m-1,n-1}^{(1)}\right)\right]\end{aligned} \tag{23}$$

$$\begin{aligned}H_k^{(m,q)}(\underline{k}_t) = 2j^{(m+1)}\frac{1}{k_t}\cos m\alpha\Bigg[&-\frac{q+2}{2}f_{m,q+2}^{(1)} \\ &- \frac{q+1}{t}f_{m,q+1}^{(1)} - \frac{q}{2}f_{m,q}^{(1)}\Bigg]\end{aligned} \tag{24}$$

$$H_\alpha^{(m,q)}(\underline{k}_t) = j^{(m+1)}\frac{2m}{k_t}\sin m\alpha\left[-\frac{1}{2}f_{m,q}^{(1)} - \frac{1}{2}f_{m,q+2}^{(1)}\right] \tag{25}$$

and

$$\begin{aligned}f_{m,r}^{(1)} &= \int_{-1}^{+1}\frac{T_r(x)}{\sqrt{1-x^2}}J_m\left(k_t w\left(x+\frac{1}{t}\right)\right)dx \\ &= \left\langle T_r(x), J_m\left(k_t w\left(x+\frac{1}{t}\right)\right)\right\rangle\end{aligned} \tag{26}$$

with $t = w/r_0$.

The integral in (26) cannot be expressed in closed form. Its calculation can be carried out via Neumann's addition formula [20] or similar procedures [15]. An alternative, efficient procedure is to evaluate $f_{m,r}^{(1)}$ as coefficients of the T-expansion of $J_m(k_t w(x+\frac{1}{t}))$; these coefficients can be evaluated via the properties of Chebyshev polynomials [21]. In this way all integrals for different r and same m are evaluated at the cost of one.

REFERENCES

[1] G. Vecchi, L. Matekovits, P. Pirinoli, and M. Orefice, "A numerical regularization of the EFIE for three-dimensional planar structures in layered media," *Int. J. Micro. Millimeter Wave Computer-Aided Eng*, Special issue on frequency-domain modeling of planar circuits and antennas, vol. 7, no. 6, pp. 410–431, Nov. 1997.

[2] ——, "Hybrid spectral-spatial method for the analysis of printed antennas," *Radio Sci. (Special Issue Computat. Electromagn.)*, vol. 31, no. 5, pp. 1263–1270, Sept.–Oct. 1996.

[3] J. P. Damiano, J. Bennegueouche, and A. Papiernik, "Study of multilayer microstrip antennas with radiating elements of various geometry," *Proc. Inst. Elect. Eng.*, vol. 137, pt. H, no. 3, pp. 163–170, June 1990.

[4] S. M. Ali, W. C. Chew, and J. A. Kong, "Vector Hankel transform analysis of annular-ring microstrip antenna," *IEEE Trans. Antennas Propagat.*, vol. AP-30, pp. 637–645, July 1982.

[5] Z. Fan and K. F. Lee, "Input impedence of annular-ring microstrip antennas with a dielectric cover," *IEEE Trans. Antennas Propagat.*, vol. 40, pp. 992–995, Aug. 1992.

[6] N. S. Nurie and R. J. Langley, "Input impedence of concentric ring microstrip antennas for dual frequency band operation including surface wave coupling," *Proc. Inst. Elect. Eng.*, vol. 137, pt. H, no. 6, pp. 331–336, Dec. 1990.

[7] L. Economou and R. J. Langley, "Hankel domain analysis of ring patch antennas for mobile communications," in *Proc. Int. Conf. Electromagn. Advanced Applicat.*, Torino, Italy, Sept. 1995, pp. 7–10.

[8] L. Economou and R. J. Langley, "Performance of ring patch antennas with glass superstrates," *Microwave Opt. Technol. Lett.*, vol. 11, no. 1, pp. 8–10, Jan. 1996.
[9] T. K. Wu and S. W. Lee, "Multiband frequency selective surface with multiring patch elements," *IEEE Trans. Antennas Propagat.*, vol. 42, pp. 1484–1489, Nov. 1994.
[10] M. Davidovitz and Y. T. Lo, "Rigorous analysis of a circular patch antenna excited by a microstrip trasmission line," *IEEE Trans. Antennas Propagat.*, vol. 37, pp. 949–958, Nov. 1994.
[11] N. Amitay and V. Galindo, "On the scalar product of certain circular and cartesian wave functions," *IEEE Trans. Microwave Theory Tech.*, vol. MTT-16, pp. 265–266, Apr. 1968.
[12] G. Vecchi, M. Orefice, C. Vai, and P. Pirinoli, "Spectral analysis of printed circular rings for use with a general coupling," in *Proc. Int. Conf. Electromagn. Advanced Applicat.*, Torino, Italy, Sept. 1995, pp. 23–26.
[13] N. Marcuvitz, *Waveguide Handbook*. New York: McGraw-Hill, 1951, Sec. 2.4.
[14] R. Orta, P. Savi, and R. Tascone, "Multiple frequency selective surfaces consisting of ring patches," *Electromagn.*, vol. 15, no. 4, pp. 417–426, July 1995.
[15] P. Pirinoli, G. Vecchi, and M. Orefice, in *Italian Recent Advances in Applied Electromagnetics*, G. Franceschetti and R. Pierri, Eds. Napoli, Italy: Liguori, 1991, pp. 181–194.
[16] G. Vecchi, P. Pirinoli, L. Matekovits, and M. Orefice, "A reduced representation of the frequency response of printed antennas," in *Proc. 25th Eur. Microwave Conf.*, Bologna, Italy, Sept. 1995, pp. 372–376.
[17] G. Vecchi, L. Matekovits, P. Pirinoli, and M. Orefice, "Application of numerical regularization options to the integral-equation analysis of printed antennas," *IEEE Trans. Antennas Propagat. (Special Issue: Numer. Tech.)*, vol. 45, pp. 570–572, Mar. 1997.
[18] G. Vecchi, M. Orefice, P. Pirinoli, and C. Vai, "Spectral analysis of printed circular rings for use with a general coupling," *Alta Frequenza*, vol. 8, no. 1, pp. 43–45, 1996.
[19] P. Pirinoli, "Full-wave analysis of printed antennas," Ph.D. dissertation, Politecnico di Torino, 1993 (in Italian).
[20] M. Abramovitz and I. A. Stegun, *Handbook of Mathematical Functions*. New York: Dover, 1972.
[21] W. H. Press, B. P. Flannery, S. A. Teukolsky, and W. T. Vetterling, *Numerical Recipes*. New York: Cambridge Univ. Press, 1990.

Giuseppe Vecchi (M'90) received the Laurea and Ph.D. (Dottorato di Ricerca) degrees in electronic engineering from the Politecnico di Torino, Torino, Italy, in 1985 and 1989, respectively.

From August 1989 to February 1990, he was a Visiting Scientist at Polytechnic University, Farmingdale, NY, through an Italian National Research Council (CNR) Fellowship. He then joined the Politecnico di Torino as a Researcher in the Department of Electronics. In November 1992, he was appointed Associate Professor of Electromagnetism. His main research activities concern analytical and numerical techniques in high- and low-frequency electromagnetics, electromagnetic compatibility, and fractal electrodynamics.

Paola Pirinoli (M'97) received the M.S. (Laurea) and Ph.D. (Dottorato di Ricerca) degrees in electronic engineering, from the Politecnico di Torino, Italy, in 1989 and 1993, respectively.

In October 1994, she joined the Politecnico di Torino as a Researcher in the Department of Electronics. From November 1996 to February 1997 she was a Visiting Research Fellow at the Laboratoire d'Electronique, Antennes et Télécomunication of the University of Nice (F), through a Fellowship of the Communauté de Travail des Alpes Occidentales (COTRAO). Her main research activities include analytically based numerical techniques, essentially applied to the study of printed structures on planar or curved substrates.

Mario Orefice (M'82) received the B.S. degree from the Politecnico di Torino, Italy, in 1968.

He is currently a Professor of electromagnetic waves and antennas at the Politecnico di Torino, Italy. He was Research Scientist of the National Research Council of Italy at the Center of Studies on Propagation and Antennas (CESPA) from 1971 to 1983, as well as an Adjunct Professor at Politecnico di Torino from 1976 to 1983. He was a Visiting Scholar at UCLA in 1979. In 1983, he became Associate Professor at Politecnico di Torino. He has been a Full Professor since 1990 and since 1992 he has been Vice-Dean of the Second School of Engineering. His technical and scientific activity has been in the area of theoretical and experimental studies on antennas and applied electromagnetics, in particular, on waveguide discontinuities, reflector antennas, waveguide arrays, and printed antennas.

Mr. Orefice is Vice Chairman of the Northern Italy Joint Chapter of AP, MTT, ED, CT, and is the General Chairman of the International Conference in Electromagnetics in Advanced Applications sponsored by IEEE and held biannually in Torino, Italy.